Large Signal Analysis of On-Chip Interconnects Using Transport Based Approach

Gaofeng Wang*, Xiaoning Qi, Zhiping Yu and Robert W. Dutton
Center for Integrated Systems
Stanford University, Stanford, CA 94305

Conor S. Rafferty
Bell Laboratories, Lucent Technologies
Murray Hill, NJ 07974

Abstract

A large signal analysis of on-chip interconnects is presented. A set of nonlinear equations combining the motion equations of charge carriers and Maxwell's equations is devised in the frequency domain for the fundamental mode and harmonics and then solved by the finite element method and Newton's iterations. This analysis provides knowledge on field-carrier interaction, substrate nonlinearity and loss, slow-wave effect, etc. Numerical examples are provided for some practical material and geometrical parameters.

Introduction

Due to denser and larger chips and higher clock rates effects of on-chip interconnects are becoming a limiting factor to the overall performance of circuits. Semiconductor substrate effects have been of fundamental interest. In order to describe the behavior of semiconductor as solid state plasma, the motion equations of charge carriers should be included in the analysis [1]. In [2], the propagation property of on-chip interconnects was studied using a parallel-plate waveguide model and a transport based analysis. The approach in [2] is, however, applicable only to small signal analysis due to its linearization of equations.

The nonlinear nature of semiconductor substrates of on-chip interconnects has been systematically ignored by most of previous research. The question when the nonlinearity can be safely neglected is, however, not answered adequately. In this paper, a device level analysis is presented to study the propagation characteristics of on-chip interconnects. The nonlinearity in the motion equations of charge carriers is included in the analysis. Thus, this approach is suitable for both small signal and large signal analyses.

Theory

An on-chip interconnect can be simply modeled as a parallel-plate metal-insulator-semiconductor (MIS) structure, as shown in Fig. 1, extending from $y=-\infty$ to $y=\infty$. For an arbitrary variable $v(\mathbf{r},t)$, one has

$$v(\mathbf{r},t)=v_0(x)+\sum_{m=1}^{\infty}v^{(m)}(x)\cdot e^{-m\gamma z}\cdot e^{jm\omega t} \qquad (1)$$

where ω is the fundamental frequency, γ is the propagation factor , $v_0(x)$ denotes the stead state solution, and $v^{(m)}(x)$ represents the m-th harmonic component. The equations for the m-th harmonic are given by

0-7803-6377-9/00/$10.00 © 2000 IEEE.

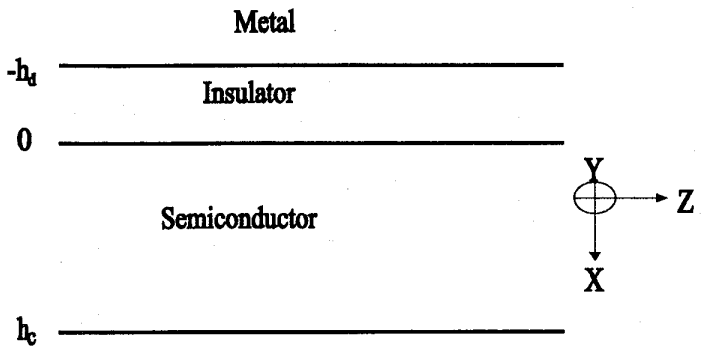

Figure 1: Configuration of a parallel-plate MIS waveguide

$$\frac{\partial^2 E_z^{(m)}(x)}{\partial x^2} + m^2\left(k_c^2 + \gamma^2\right)E_z^{(m)}(x) = jm\omega\mu\left[J_{nz}^{(m)(r)}(x) + J_{pz}^{(m)(r)}(x)\right] - \frac{qm\gamma}{\varepsilon}\left[p^{(m)}(x) - n^{(m)}(x)\right] \tag{2.a}$$

$$jm\omega\, n^{(m)}(x) = \frac{1}{q}\frac{\partial J_{nx}^{(m)}(x)}{\partial x} - \frac{m\gamma}{q}J_{nz}^{(m)}(x) - u^{(m)}(x) \tag{2.b}$$

$$jm\omega\, p^{(m)}(x) = -\frac{1}{q}\frac{\partial J_{px}^{(m)}(x)}{\partial x} + \frac{m\gamma}{q}J_{pz}^{(m)}(x) - u^{(m)}(x) \tag{2.c}$$

$$E_x^{(m)}(x) = \frac{-m\gamma}{m^2\left(k^2+\gamma^2\right)}\left\{\frac{\partial E_z^{(m)}(x)}{\partial x} - \frac{j\omega\mu\left[J_{nx}^{(m)}(x) + J_{px}^{(m)}(x)\right]}{\gamma}\right\} \tag{2.d}$$

$$H_y^{(m)}(x) = \frac{1}{jm\omega\mu}\left[\frac{\partial E_z^{(m)}(x)}{\partial x} + m\gamma E_x^{(m)}(x)\right] \tag{2.e}$$

where

$$\left(1 + jm\omega\tau_n\right)\mathbf{J}_n^{(m)(0)}(x) = q\mu_n\, n_0(x)\mathbf{E}^{(m)}(x) \tag{3.a}$$

$$\left(1 + jm\omega\tau_p\right)\mathbf{J}_p^{(m)(0)}(x) = q\mu_p\, p_0(x)\mathbf{E}^{(m)}(x) \tag{3.b}$$

$$\left(1 + jm\omega\tau_n\right)\mathbf{J}_n^{(m)}(x) = q\mu_n\sum_{s=0}^{m}\left[n^{(s)}(x)\mathbf{E}^{(m-s)}(x)\right] + qD_n\nabla n^{(m)}(x) - \hat{\mathbf{z}}\, qD_n m\gamma n^{(m)}(x) \tag{3.c}$$

$$\left(1 + jm\omega\tau_p\right)\mathbf{J}_p^{(m)}(x) = q\mu_p\sum_{s=0}^{m}\left[p^{(s)}(x)\mathbf{E}^{(m-s)}(x)\right] - qD_p\nabla p^{(m)}(x) + \hat{\mathbf{z}}\, qD_p m\gamma\, p^{(m)}(x) \tag{3.d}$$

$$\mathbf{J}_n^{(m)(r)}(x) = \mathbf{J}_n^{(m)}(x) - \mathbf{J}_n^{(m)(0)}(x),\ \mathbf{J}_p^{(m)(r)}(x) = \mathbf{J}_p^{(m)}(x) - \mathbf{J}_p^{(m)(0)}(x) \tag{3.e}$$

$$k_c^2 = k^2 - \frac{j\omega\mu\, q}{m}\left[\frac{\mu_n n^{(0)}(x)}{1 + jm\omega\tau_n} + \frac{\mu_p p^{(0)}(x)}{1 + jm\omega\tau_p}\right] \tag{3.f}$$

where $\mathbf{E}$ and $\mathbf{H}$ are, respectively, the electric and magnetic fields, ε and μ are, respectively, the permittivity and permeability of the semiconductor, p and n are, respectively, the hole and electron density, q is the elementary charge, $\mathbf{J}_n$ and $\mathbf{J}_p$ are, respectively, the electron and hole current densities, u is the total net recombination rate, μ_n and μ_p are, respectively,

effective carrier mobility of electrons and holes, D_n and D_p are, respectively, diffusion coefficient for electrons and holes, and τ_n and τ_p are, respectively, average collision times of electrons and holes.

The boundary conditions are as follows:

$$E_z^{(m)}(0) = -A^{(m)} k_d \sin(mk_d h_d)/\gamma \tag{4.a}$$

$$H_y^{(m)}(0) = j\omega\varepsilon_d A^{(m)} \cos(mk_d h_d)/\gamma \tag{4.b}$$

$$J_{nx}^{(m)}(0) = J_{px}^{(m)}(0) = E_z^{(m)}(h_c) = n^{(m)}(h_c) = p^{(m)}(h_c) = 0 \tag{4.c}$$

where ε_d and μ_d are, respectively, the permittivity and permeability of the insulator, and $k_d = \sqrt{\omega^2\mu_d\varepsilon_d + \gamma^2}$. The artificial boundary at $x = h_c$ is usually made to be far away from the signal line so that its actual location has little impact on the propagation characteristics.

For the fundamental mode, eliminating the arbitrary constant $A^{(1)}$ in (4.a) and (4.b) leads to

$$E_z^{(1)}(0)/H_y^{(1)}(0) = -k_d \tan(k_d h_d)/j\omega\varepsilon_d \tag{5}$$

Equation (5) provides a nonlinear algebraic equation for determining the propagation factor γ. For a high order harmonic, (4.b) and (2.e) are compatible only if

$$E_z^{(m)}(0)/H_y^{(m)}(0) = -mk_d \tan(mk_d h_d)/jm\omega\varepsilon_d \tag{6}$$

or

$$A^{(m)} = 0 \tag{7}$$

The propagation factor γ determined from (5) hardly meets condition (6). Thus, condition (7) must be imposed as the compatibility condition. Condition (7) implies that high order harmonics due to the nonlinearity are confined in the semiconductor and do not penetrate into the insulator. Since the equations are nonlinear in γ, it is essentially a nonlinear system, which can be solved by the finite element method [3] and Newton's method [4].

Numerical Results

For the examples below, the following parameters were assumed: $\mu_n = 1500\ \mathrm{cm^2/(v\cdot s)}$, $\mu_p = 450\ \mathrm{cm^2/(v\cdot s)}$, $\varepsilon = 11.9\varepsilon_0$, $\varepsilon_d = 3.9\varepsilon_0$, $\mu = \mu_d = \mu_0$, $T = 300\mathrm{K}$, $h_d = 0.05\mu\mathrm{m}$, and $h_c = 100\mu\mathrm{m}$, where ε_0 and μ_0 are, respectively, the permittivity and permeability in vacuum. The semiconductor was assumed to be *n*-type silicon.

Figs. 2-3 illustrate the transverse field components for the fundamental mode and the second order harmonic at a fundamental frequency $f = 5\mathrm{GHz}$, when an excitation with $A^{(1)} = 10^4\ \mathrm{v/cm}$ and a positive external bias +0.1v were applied. The normalized phase constant β/k_0 is obtained as 65.8303 and the attenuation constant as 25.5191 dB/mm, where k_0 denotes the wave number in vacuum. The large normalized phase constant indicates that the MIS structure supports a slow wave. Moreover, the attenuation constant directly accounts for the semiconductor loss.

This analysis shows a strong coupling effect between $E_x^{(1)}$ and charge carriers, which leads to a different solution in the accumulation-depletion layer from that predicted by the uniform conductivity model. As indicated in the plots, the screening effect of the carriers

near the accumulation-depletion layer prevents the electrical field from penetrating the semiconductor to beyond a few Debye lengths.

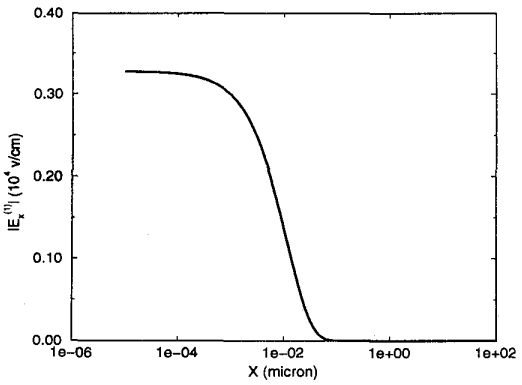

Figure 2: Magnitude of $E_x^{(1)}$ in the semiconductor substrate

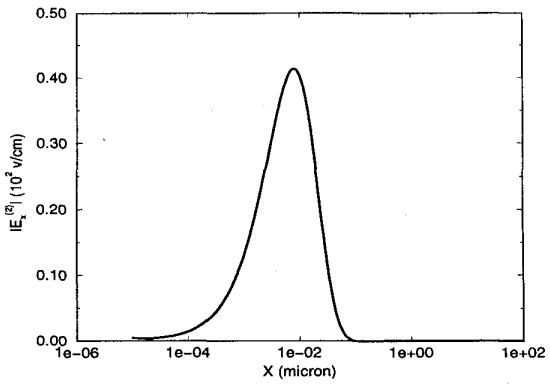

Figure 3: Magnitude of $E_x^{(2)}$ in the semiconductor substrate

Moreover, this analysis is capable of predicting harmonics quantitatively, as shown in Fig. 3. It can be shown that the fundamental mode is linearly proportional to the excitation magnitude $A^{(1)}$. Using the fact, the fundamental mode for the excitation with $A^{(1)} = 10^{-2}$ v/cm can readily obtained by scaling Fig. 2 with a factor 10^{-6}, which gives results in a close agreement with that from the small signal analysis, i.e., Fig. 6 of [2]. Moreover, numerical calculation reveals that the second harmonic is proportional to $\left[A^{(1)}\right]^2$. When the excitation gets larger, the nonlinearity becomes more severe.

Conclusion

A large signal analysis has been presented for studying on-chip interconnects using transport equations and Maxwell's equations. This approach is capable of studying field-carrier interaction, semiconductor loss and nonlinearity, slow-wave effect, and external bias effect. It has been shown that the high order harmonics due to the nonlinearity are confined in the semiconductor and do not penetrate into the insulator.

References

[1] C. M. Krowne and G. B. Tait, "Propagation in layered biased semiconductor structures based on transport analysis," *IEEE Trans. Microwave Theory Tech.*, vol.MTT-37, pp.711-722, April 1989.

[2] K. Han and T. T. Y. Wong, "Space-charge wave considerations in MIS waveguide analysis," *IEEE Trans. Microwave Theory Tech.*, vol.MTT-39, pp.1126-1132, July 1991.

[3] T. J. R. Hughes, *The Finite Element Method: Linear Static and Dynamic Finite Element Analysis*. Englewood Cliffs, NJ: Prentice-Hall, 1987.

[4] J. E. Dennis and R. B. Schnabel, *Numerical Methods for Unconstrained Optimization and Nonlinear Equations*. Englewood Cliffs, NJ: Prentice-Hall, 1983.